Evaluation of elastic modulus of carbon fiber reinforced polymers using an optical extensometer

Lyubutin P S[1,a], Burkov M V[1,2] and Eremin A V[1,2]

[1] Institute of Strength Physics and Materials Science, Akademicheskiy avenue 2/4, Tomsk, 634055, Russia
[2] Tomsk Polytechnic University, Lenin avenue 30, Tomsk, 634050, Russia

[a)]Corresponding author: burkovispms@mail.ru

Abstract. The paper presents the results of application of different techniques for processing of digital image correlation data. The algorithms are described and applied for determination of elasticity modulus of carbon fiber reinforced polymer specimens tested by uniaxial tension. Two ways of evaluation of elongation along with two methods of elastic modulus calculation resulted in four techniques which have shown quite similar results with a scatter of 0.5-2%.

1. Introduction

Evaluation of the properties of materials during their mechanical testing is an urgent task. Optical systems based on digital image correlation method make it possible to measure strains in a non-contact way with high accuracy [1-3]. Optical extensometers based on the digital image correlation method have been developed [4–9]. In [10], the accuracy of an optical extensometer is evaluated in comparison with a strain gauge, as well as a comparison of 2D and 3D optical extensometer. It is shown that 2D systems are not enough for real tests of materials. In our paper, the principle of evaluating the elastic properties of materials using a system of stereo imaging and the method of digital image correlation is considered.

2. Mathematics

Motion detection in Digital Image Correlation Method (DIC) on a series of images in a general form is based on minimizing the functional

$$E(w,S) = E_D(w,S) + \alpha E_S(w,S), \quad (1)$$

where w is the shape function, S is the image area over which E is minimized, E_D is the similarity measure of image blocks, E_S is the similarity measure of vectors in the optical stream, and α is the regularization coefficient.

The similarity measures E_D of two sections of the current image (CI) and the reference image (RI) can be determined by various functions, the condition of which is the presence of an extremum, usually a minimum. The simplest measure of proximity is the sum of the squared difference [11]:

$$SSD = \sum_{X \in S}\big(F(X) - G(X,w)\big)^2, \quad (2)$$

where $F(X)$, $G(X,w)$ are the brightness of the pixels of the compared sections of CI and RI, respectively, X is the coordinate of the pixels of the section S, w is the shape function.

One of the most difficult measures is the normalized sum of squared difference with zero mean [12,13]:

$$ZNSSD = \sum_{X\in S}\left(\frac{F(X)-\bar{F}}{\sqrt{\sum_{X\in S}(F(X)-\bar{F})^2}} - \frac{G(X,w)-\bar{G}}{\sqrt{\sum_{X\in S}(G(X,w)-\bar{G})^2}}\right)^2, \quad (3)$$

where $\bar{F}$ and $\bar{G}$ are arithmetic mean values of the CI and RI images, respectively.

There are two ways to find the minimum functional *E*:

- Block method. The reference image area *S* is compared in a sliding window with the current image. Often this approach is used to pre-search for large movements with pixel accuracy. However, it is rarely used in calculations with subpixel accuracy and with a complex shape function, because it leads to unreasonably large computational costs;
- Application of optimization. Any numerical optimization algorithm is used, for example, the Newton-Raphson or Gauss-Newton algorithm. The optimization approach, on the contrary, is used in the subpixel region, since it provides stable convergence in the range of [−1 ÷ +1] pixel.

Newton-Raphson optimization [14,15] can be written as follows:

$$P^{k+1} = P^k - \frac{\nabla E(P^k)}{\nabla\nabla E(P^k)} \quad (4)$$

where *k* is the iteration number, *p* is the parametric vector containing the coefficients of the form function.

The system of equations describing the displacements in the region *S*, based on the affine shape function, has the following form [15,16]:

$$\begin{cases} \tilde{x}(x,y) = p_0 + p_2 x + p_4 y \\ \tilde{y}(x,y) = p_1 + p_3 x + p_5 y \end{cases} \quad (5)$$

In the case of using a stereo vision system, processing of stereo pairs of images is required to determine the spatial coordinates of points on the surface of an object. Initially a calibration is carried out to determine the parameters of individual cameras and the system as a whole for the installed stereo vision system. The parameters contain the matrix of projective transformations of the object on the plane of the cameras, distance, angle between the planes of the cameras, etc. The reconstruction of three-dimensional coordinates for the points of the stereo pair is carried out by calculating the disparity map, which reflects the displacement of the image points of the right camera relative to the left. The determination of disparity maps is carried out by the algorithms considered above. The obtained spatial coordinates of the points are recalculated into displacements corresponding to the given values of the loading of the sample. The set of points forms the spatial field of the displacement vectors of the sample surface.

In the paper two extensometer algorithms were used to assess the strain:

- Determination of elongation of the specimen between two points (gagelength);
- Integrated strain assessment of the whole specimen.

The elongation of the sample between two points (p1 and p2) is defined as the difference between the two Euclidean distances before and after application of the load. The deformation is calculated as follows:

$$\varepsilon = \frac{L_i - L_0}{L_0}, \quad L_0 = \sqrt{(x_2-x_1)^2 + (y_2-y_1)^2 + (z_2+z_1)^2},\ L_i = \sqrt{(x_2'-x_1')^2 + (y_2'-y_1')^2 + (z_2'-z_1')^2}, \quad (6)$$

where (x_1,y_1,z_1), (x_2,y_2,z_2) are coordinates of the points of the extensometer before loading, (x'_1,y'_1,z'_1), (x'_2,y'_2,z'_2) are coordinates of the points of the extensometer after loading.

An integral estimate of the strain over a region implies an approximation of the field of displacement vectors converted to local coordinates and differentiation of the resulting function. The surface of the sample is approximated by a function; a biquadratic function was used in the work:

$$z(x,y) = \sum_{i=0}^{2}\sum_{j=0}^{2} a_{ij}(x-x_c)^i(y-y_c)^j \quad (7)$$

where x_c, y_c are the coordinates of the center point of the sample or region of interest highlighted on the sample.

The field of displacement vectors is approximated using trilinear approximation:

$$U(x,y,z) = U_0 + U_1x + U_2y + U_3z + U_4xy + U_5xz + U_6yz + U_7xyz,$$
$$U_0 = \begin{bmatrix} u_0 \\ v_0 \end{bmatrix} \dots U_7 = \begin{bmatrix} u_7 \\ v_7 \end{bmatrix}, x = x - x_c, y = y - y_c, z = z - z_c \quad (8)$$

where u_i, v_i, i=0..7 are trilinear approximation coefficients.

Since the differentiation on the surface is considered, by substituting $z(x,y)$ in $U(x,y,z)$, the function U depending only on two coordinates (x,y) is obtained. The final function is bicubic.

$$U(x,y) = U_0 + U_1x + U_2y + U_3z(x,y) + U_4xy + U_5xz(x,y) +$$
$$U_6yz(x,y) + U_7xyz(x,y) = \sum_{i=0}^{3}\sum_{j=0}^{3} U'_{ij}(x-x_c)^i(y-y_c)^j \; ; \; U'_{ij} = \begin{bmatrix} u'_{ij} \\ v'_{ij} \end{bmatrix} \quad (9)$$

where u'_{ij}, v'_{ij} are the approximation coefficients of the vector field.

The strain tensor values are obtained by differentiating the function $U(x,y)$ at the point (x_c,y_c)

$$\varepsilon_{xx} = \frac{\partial u(x_c,y_c)}{\partial x} = u'_{10}; \varepsilon_{yy} = \frac{\partial v(x_c,y_c)}{\partial y} = v'_{01}; \varepsilon_{xy} = 0.5\left(\frac{\partial u(x_c,y_c)}{\partial y} + \frac{\partial v(x_c,y_c)}{\partial x}\right) = 0.5(u'_{01} + v'_{10}) \quad (10)$$

The elastic modulus was calculated by two methods:

- As the ratio of stress increment and strain taken between two points;
- Using a linear approximation of stress-strain points.

3. Materials and testing technique

The specimens for testing were carbon fiber reinforced polymers (CFRP) prepared according to ASTM D3039M-14 with a balanced symmetric pseudosotropic lay-up $[0/90;+45/-45]_{4S}$. CBX300 biaxial fabrics made of PAN carbon fiber Mitsubishi Pyrofil TR50S 12K was used along with R&G Epoxy L with GL2 hardener to prepare blanks. The specimens with sizes of 250 x 25 x 4 mm were cut from blanks and tested using Instron 5582 with a loading rate of 3 mm/min.

The speckle was applied to the specimen surface in imaged during tensile testing. The experimental stereo vision system included two Canon EOS 700D digital cameras (CMOS sensor resolution is 5184×3456 pixels with a physical size of 22.3×14.9 mm). The imaging was synchronized using a computer-controlled hardware trigger.

4. Experimental results and discussion

Tensile elongation of the tested CFRP specimens exceeds 6000 με thus according to ASTM D3039M-14 the elastic modulus was determined in the range from $0.25\varepsilon_{max}$ to $0.5\varepsilon_{max}$ (figure 1). ε_{max} was defined as the strain corresponding to the maximum tensile stress achieved during testing.

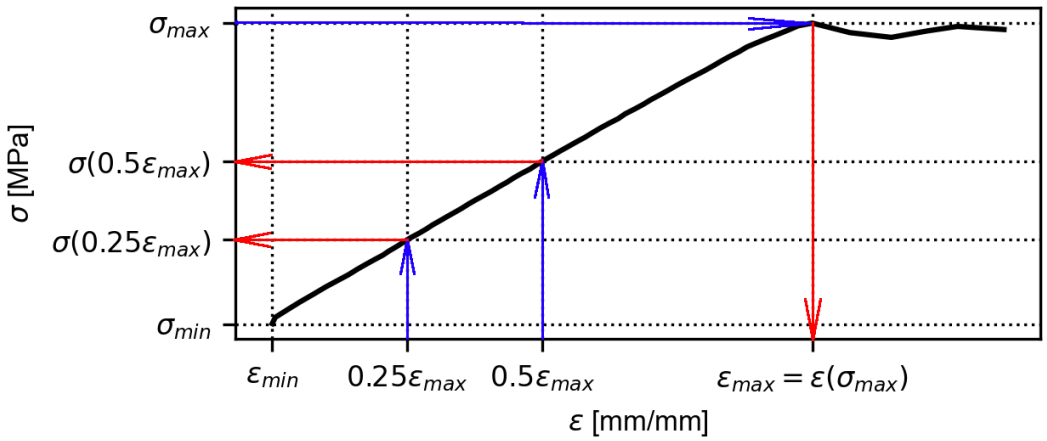

Figure 1. Typical strain-stress plot with defined limits for elastic modulus calculation.

The elastic modulus was determined by the four described methods (table 1, figure 2a). The description of alphanumeric designations is following:

- e_{2p} is 2 point-extensometer;
- e_{fit} is an extensometer based on fitting a strain field of displacement vectors;
- EM_{2p} is 2 point elastic modulus approximation (according to the technique proposed in ASTM D30309M-14);
- $EM_{fitting}$ is a calculation of elastic modulus based on linear fitting.

For all specimens except ST2 all four methods demonstrate similar modulus values. The deviation between the values for different methods is in the range of 307–1235 MPa. For ST2, the maximum deviation between the module values is observed and equals 2267 MPa. This is explained by the deviation from the linear dependence of the σ-ε plot obtained using DIC analysis (figure 2b), which is probably due to errors during the DIC data acquisition. Also it can be seen from the results that the 1st blank has lower mechanical properties than 2nd and 3rd. It has been also confirmed by similar dependence of the ultimate tensile strength obtained after tensile testing.

Table 1. Elastic modulus calculated by different methods.

CFRP blank	Specimen	Elastic modulus, MPa			
		e_{2p}/EM_{2p}	$e_{2p}/EM_{fitting}$	e_{fit}/EM_{2p}	$e_{fit}/EM_{fitting}$
1	ST1	55315	55093	55740	55632
1	ST2	53587	56008	52929	55860
2	ST3	60491	59832	59390	59399
2	ST4	59834	59645	60163	60073
3	ST5	57946	58157	59140	59142
3	ST6	57157	57193	57385	57315

5. Conclusion

The experimental testing of the technique for calculation of elasticity modulus has been performed using CFRP specimens. There were 4 methods combining two ways of elongation evaluation and two data fitting techniques. All proposed methods give similar results of elasticity modulus determination with a slight deviation from each other. Calculation of the elastic modulus using linear approximation in combination with an integrated estimate of the strain over the strain filed shows a more stable result.

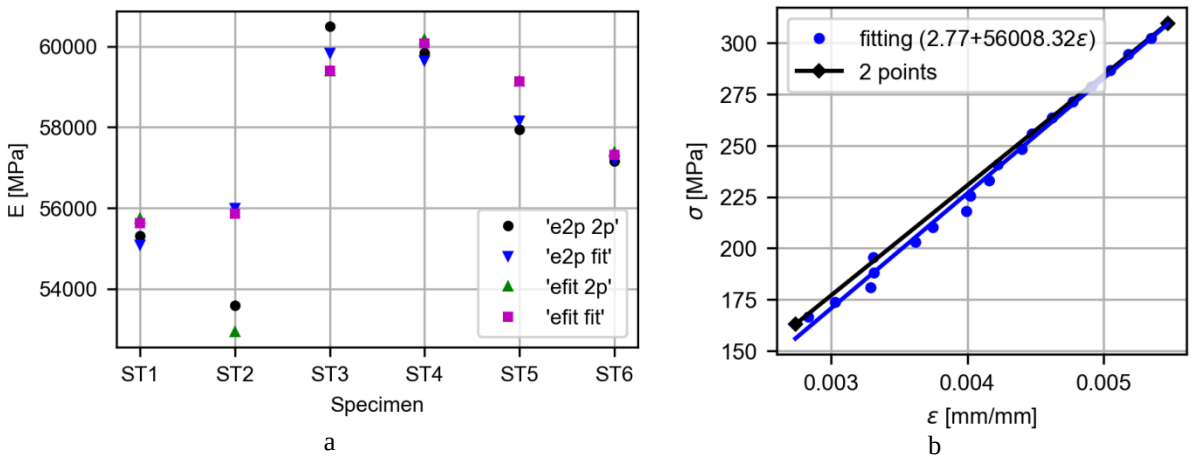

Figure 2. Elastic modulus depending on the specimen for various calculation methods (a) and two calculation methods for the specimen ST2 (b)

Acknowledgements

The investigation of data processing techniques was performed in the framework of fundamental research Program of the Russian State Academies of Sciences for 2013–2020, line of research III.23.1.3 and was funded by RFBR and the Administration of Tomsk Region according to the research project № 18-47-700006. The preparation of the specimens and tensile testing was supported by Grant of Russian Science Foundation №19-79-10148.

References

[1] Jerabek M, Major Z and Lang R W 2010 Strain determination of polymeric materials using digital image correlation *Polym. Test.* **29** 407–16
[2] Heinz S R and Wiggins J S 2010 Uniaxial compression analysis of glassy polymer networks using digital image correlation *Polym. Test.* **29** 925–32
[3] Sun P-Y, Zhu Z-K, Su C-Y, Lu L, Zhou C-Y and He X-H 2019 Experimental characterisation of mechanical behaviour for a TA2 welded joint using digital image correlation *Opt. Lasers Eng.* **115** 161–71
[4] Pan B and Tian L 2016 Advanced video extensometer for non-contact, real-time, high-accuracy strain measurement *Opt. Express* **24** 19082–93
[5] Hild F and Roux S 2006 Digital Image Correlation: from Displacement Measurement to Identification of Elastic Properties - a Review *Strain* **42** 69–80
[6] Zhu F, Bai P, Gong Y, Lei D and He X 2018 Accurate measurement of elastic modulus of specimen with initial bending using two-dimensional DIC and dual-reflector imaging technique *Measurement* **119** 18–27
[7] Tian L, Yu L and Pan B 2018 Accuracy enhancement of a video extensometer by real-time error compensation *Opt. Lasers Eng.* **110** 272–8
[8] Zhu F, Gong Y, Bai P, Jiang Z and Lei D 2017 High-accuracy biaxial optical extensometer based on 2D digital image correlation *Meas. Sci. Technol.* **28** 085006
[9] Dong B, Tian L and Pan B 2019 Tensile testing of carbon fiber multifilament using an advanced video extensometer assisted by dual-reflector imaging *Measurement* **138** 325–31
[10] Shao X, Eisa M M, Chen Z, Dong S and He X 2016 Self-calibration single-lens 3D video extensometer for high-accuracy and real-time strain measurement *Opt. Express* **24** 30124–38
[11] Giachetti A 2000 Matching techniques to compute image motion *Image Vis. Comput.* **18** 247–60
[12] Tong W 2005 An evaluation of digital image correlation criteria for strain mapping applications *Strain* **41** 167–75
[13] Pan B, Xie H, Guo Z and Hua T 2007 Full-field strain measurement using a two-dimensional Savitzky-Golay digital differentiator in digital image correlation *Opt. Eng.* **46** 33601–10
[14] Bruck H A, McNeill S R, Sutton M A and Peters W H 1989 Digital image correlation using Newton-Raphson method of partial differential correction *Exp. Mech.* **29** 261–7
[15] Cofaru C, Philips W and Van Paepegem W 2010 Improved Newton–Raphson digital image correlation method for full-field displacement and strain calculation *Appl. Opt.* **49** 6472
[16] Schreier H, Orteu J-J and Sutton M A 2009 *Image Correlation for Shape, Motion and Deformation Measurements* (Boston, MA: Springer US)